Journal of Statistical Physics, Vol. 39, Nos. 1/2, 1985

Spectrum of Certain Non-Self-Adjoint Operators and Solutions of Langevin Equations with Complex Drift

John R. Klauder[1] **and Wesley P. Petersen**[1]

Received July 6, 1984; revised October 29, 1984

As part of a program to evaluate expectations in complex distributions by long-term averages of solutions to Langevin equations with complex dirft, a simple one-dimensional example is examined in some detail. The validity and rate of convergence of this scheme depends on the spectrum of an associated non-self-adjoint Hamiltonian which is found numerically. In the regime where the stochastic evaluation should be accurate numerical solution of the Langevin equation shows this to be the case.

KEY WORDS: Diffusion; complex drift; non-self-adjoint Hamiltonian; Langevin equation; numerical solutions.

1. INTRODUCTION

1.1. Preliminaries

Consider the Fokker–Planck equation (forward Kolmogorov equation)[1] given by

$$\frac{\partial F(x,t)}{\partial t} = \frac{1}{2}\frac{\partial}{\partial x}\left[\frac{\partial}{\partial x} + \frac{\partial S(x)}{\partial x}\right] F(x,t) \tag{1}$$

for $t \geqslant 0$ subject to the initial condition $F(x,0) = F_0(x)$. For $S(x)$ a smooth real function with the property that $e^{-S(x)}$ is integrable, it follows that

$$\lim_{t\to\infty} F(x,t) = Ce^{-S(x)} \tag{2}$$

[1] AT&T Bell Laboratories, Murray Hill, New Jersey 07974.

0022-4715/85/0400-0053$04.50/0

for all smooth initial distribution F_0. Here C is a constant determined so that

$$\int F(x, t)\, dx = \int F_0(x)\, dx = C \int e^{-S(x)}\, dx \tag{3}$$

The validity of (2) follows readily if we introduce

$$G(x, t) \equiv F(x, t) e^{(1/2)S(x)} \tag{4}$$

and note that

$$\begin{aligned} \frac{\partial G(x, t)}{\partial t} &= -HG(x, t) \\ &= \frac{1}{2}\left(\frac{\partial}{\partial x} - \frac{1}{2}\frac{\partial S}{\partial x}\right)\left(\frac{\partial}{\partial x} + \frac{1}{2}\frac{\partial S}{\partial x}\right) G(x, t) \\ &= -\left[-\frac{1}{2}\frac{\partial^2}{\partial x^2} + V(x)\right] G(x, t) \end{aligned} \tag{5}$$

where

$$V(x) \equiv \frac{1}{8}\left[\frac{\partial S(x)}{\partial x}\right]^2 - \frac{1}{4}\frac{\partial^2 S(x)}{\partial x^2} \tag{6}$$

It is evident that H is a self-adjoint operator with a nonnegative spectrum. Indeed if $S(x) \geqslant \text{const} + \alpha x^2$ for some $\alpha > 0$, as we shall assume, then the spectrum of H is purely discrete. Consequently,

$$\begin{aligned} G(x, t) &= \sum_{n=0}^{\infty} a_n \psi_n(x) e^{-\lambda_n t} \\ &= Ce^{-(1/2)S(x)} + \sum_{n=1}^{\infty} a_n \psi_n(x) e^{-\lambda_n t} \end{aligned} \tag{7}$$

where

$$H\psi_n(x) = \lambda_n \psi_n(x) \tag{8}$$

and we have noted that $e^{-(1/2)S}$ is an eigenfunction of zero energy, $\lambda_0 = 0$. Since $e^{-(1/2)S}$ is nowhere vanishing it is the (nondegenerate) ground state of H, and thus $\lambda_n > 0$, for all $n \geqslant 1$. Indeed we mean by this that $\lambda_n \geqslant \lambda_{\min} > 0$ for all $n \geqslant 1$. As $t \to \infty$ it follows that

$$\lim_{t \to \infty} G(x, t) = Ce^{-(1/2)S(x)} \tag{9}$$

and therefore

$$\lim_{t \to \infty} F(x, t) = Ce^{-S(x)} \tag{10}$$

as was to be shown.

We note in addition that associated to every Fokker–Planck equation is a Langevin equation (stochastic differential equation)[1] given in the present case by

$$\dot{x}(t) = -\frac{1}{2} \frac{\partial S(x)}{\partial x}\bigg|_{x = x(t)} + \xi(t) \tag{11}$$

Here ξ denotes a generalized, standard Gaussian white noise process for which

$$\langle \xi(t) \rangle = 0$$

$$\langle \xi(t_1)\, \xi(t_2) \rangle = \delta(t_1 - t_2)$$

where $\langle \cdot \rangle$ denotes an average over the white noise ensemble. If the distribution of initial values of $x(0)$ for (11) is given by F_0, then it follows for any suitable function A that

$$\langle A(x(t)) \rangle = \frac{\int A(x)\, F(x, t)\, dx}{\int F(x, t)\, dx} \tag{12}$$

Thus if

$$\bar{A} \equiv \frac{\int A(x) e^{-S(x)}\, dx}{\int e^{-S(x)}\, dx} \tag{13}$$

we see that

$$\lim_{t \to \infty} \langle A(x(t)) \rangle = \bar{A} \tag{14}$$

Moreover, the convergence criterion (2) also ensures that the ensemble is ergodic in the sense that

$$\lim_{T \to \infty} \frac{1}{T} \int_0^T A(x(t))\, dt = \bar{A} \tag{15}$$

1.2. Can S Be Complex?

In this paper we raise the question: Provided $\int e^{-S(x)}\, dx \neq 0$ and $\int |e^{-S(x)}|\, dx < \infty$, how much of the foregoing scenario remains true if S is

complex? That is, when S is complex is it possible that a general solution to the complex Fokker–Planck equation satisfies (2), and, as a consequence thereof, that solutions to the complex Langevin equation fulfill (14) and (15)? We are led to ask this question as it has recently arisen in the course of studying complex Langevin equations as a means to calculate statistical averages.[2,3]

When S is complex, the operator H defined by (5) and (6) is non-self-adjoint and nonnormal. There is a conspicuous absence of general spectral theorems in this case. If we assume that $V_i \equiv \operatorname{Im} V(x)$ is a Kato-tiny perturbation[4] of $H_r \equiv H - iV_i$, namely, for general ψ that

$$\left(\int |V_i\psi|^2\, dx\right)^{1/2} \leqslant a\left(\int |\psi|^2 dx\right)^{1/2} + b\left(\int |H_r\psi|^2\, dx\right)^{1/2} \tag{16}$$

for some positive a and b, $b<1$, then it follows from properties of the resolvent operator that eigenfunctions exist and are complete, and that both eigenfunctions and eigenvalues are analytic in the coefficient of V_i about zero. This desirable situation may always be arranged, at least for polynomial S, by analytic continuation in the independent variable x if need be. The solutions to the eigenvalue equation (again taken discrete),

$$H\psi_n(x) = \lambda_n \psi_n(x) \tag{17}$$

involve complex eigenvalues λ and eigenfunctions ψ, which need not be mutually orthogonal. Orthogonality in the form $\int \psi_n(x)\, \psi_m(x)\, dx = 0$ whenever $\lambda_n \neq \lambda_m$ does hold, however, in the present case since $\int \psi_n(x)\, H\psi_m(x)\, dx = \int \psi_m(x)\, H\psi_n(x)\, dx$ holds by integration by parts. By construction, $e^{-(1/2)S(x)}$ is always an eigenfunction with eigenvalue zero ($\lambda_0 = 0$). Consequently, the convergence criterion (2) will be fulfilled provided

$$\operatorname{Re} \lambda_n \geqslant c > 0, \qquad n \geqslant 1 \tag{18}$$

This condition would follow immediately from the Feynman–Kac formula,[5] for example, if only

$$H_r \equiv -\frac{1}{2}\frac{\partial^2}{\partial x^2} + \operatorname{Re} V(x) \tag{19}$$

was nonnegative, but this is generally not the case.

Choose S complex and assume (18) is true so that the asymptotic behavior (2) holds. Despite appearances the solutions of (11) diverge on only a set of measure zero (see the example below). Moreover, it is

straightforward to show that (1) and (11) are still linked by (12). However, the left side of (12) involves cancellation among large numbers (see below) that could be a source of error in a numerical solution of (11). In our calculation we have taken a simple approach to this problem by cutting from a given sample those paths which are growing very large in absolute value. Clearly such cutting could affect the averaging procedure, but we find that if done symmetrically about the mean of x, the results are quite stable and relatively independent of the cutting size.

To illustrate our ideas and to study these general questions further, let us specialize to a "typical" example where

$$S(x) = \sigma x^2 + \tfrac{1}{2}x^4 \tag{20}$$

and σ is a complex parameter. In this case

$$H = -\frac{1}{2}\frac{\partial^2}{\partial x^2} + \frac{1}{2}\sigma^2 x^2 - \frac{3}{2}x^2 + \sigma x^4 + \frac{1}{2}x^6 - \frac{1}{2}\sigma \tag{21}$$

In the next section we discuss the numerical results for the spectrum of the operator in (21), and show that (18) holds whenever (i) $\operatorname{Re}\sigma > 0$, or (ii) $\operatorname{Re}\sigma < 0$ provided $|\operatorname{Im}\sigma|$ is sufficiently small. The associated Langevin equation for $t \geqslant 0$ reads in this case

$$\dot{z}(t) = -\sigma z(t) - z^3(t) + \xi(t) \tag{22}$$

subject to the real initial value $z(0) = x_0$, where x_0 has a suitable distribution. Despite appearances the solutions to this equation diverge in a finite time for only a set of measure zero. If at $t = t_0$, z is large in absolute magnitude then (22) reduces essentially to $\dot{z}(t) = -z^3(t)$ the solution of which is given for $t \geqslant t_0$ by

$$z(t) \equiv x(t) + iy(t) = \pm 1/(2t - \alpha - i\beta)^{1/2} \tag{23}$$

where α and β are real. If $\beta = 0$ and $2t_0 - \alpha > 0$, then $z(t)$ approaches the origin along the x axis, while if $2t_0 - \alpha < 0$, then $z(t)$ diverges in a finite time along the y axis. However, when σ is complex, $\beta = 0$ occurs with probability zero. When $\beta \neq 0$ the solution (23) remains *finite* while traversing the outline of one of the leaves of a four-leaf clover pattern, outward from the origin when near the y axis and then inward toward the origin when near the x axis. For $\alpha = T$ and $0 < |\beta| \ll T$ the contribution to $|T^{-1}\int_0^T z^2(t)\,dt|$ of the solution (23) is given approximately by $(\pi/2T)$, while the contribution to $T^{-1}\int_0^T |z(t)|^2\,dt$ is given approximately by $(\ln(T/|\beta|)/T$. This estimate illustrates the cancellation among large numbers that is involved in (12), and higher moments show that an ever increasing

Table I. Comparison of Long-Time Average (15) to Numerical integration of (13) for $A(x) = x^2$ [a]

	Long time SDE vs. numerical integration	
σ	$\frac{1}{T}\int_0^T x^2(t)\,dt$	$\frac{\int_{-\infty}^{\infty} x^2 e^{-S(x)}\,dx}{\int_{-\infty}^{\infty} e^{-S(x)}\,dx}$
2	(0.195 ± 0.015)	0.197
$2+(1/2)i$	$(0.194 \pm 0.013) - (0.032 \pm 0.003)i$	$0.193 - 0.032i$
$2+i$	$(0.177 \pm 0.014) - (0.061 \pm 0.007)i$	$0.179 - 0.061i$
$2+2i$	$(0.134 \pm 0.009) - (0.097 \pm 0.009)i$	$0.136 - 0.099i$
$2+3i$	$(0.091 \pm 0.007) - (0.104 \pm 0.011)i$	$0.091 - 0.108i$
$2+4i$	$(0.059 \pm 0.006) - (0.099 \pm 0.010)i$	$0.059 - 0.100i$
1	(0.285 ± 0.023)	0.290
$1+(1/2)i$	$(0.280 \pm 0.020) - (0.061 \pm 0.006)i$	$0.279 - 0.062i$
$1+i$	$(0.247 \pm 0.019) - (0.114 \pm 0.012)i$	$0.248 - 0.114i$
$1+2i$	$(0.160 \pm 0.014) - (0.167 \pm 0.018)i$	$0.160 - 0.166i$
$1+3i$	$(0.079 \pm 0.014) - (0.150 \pm 0.021)i$	$0.079 - 0.155i$
$1+4i$	$(0.044 \pm 0.013) - (0.133 \pm 0.023)i$	$0.040 - 0.126i$
1/2	(0.359 ± 0.030)	0.366
$1/2+(1/4)i$	$(0.361 \pm 0.027) - (0.046 \pm 0.005)i$	$0.362 - 0.045i$
$1/2+(1/2)i$	$(0.349 \pm 0.027) - (0.087 \pm 0.009)i$	$0.349 - 0.089i$
$1/2+(3/4)i$	$(0.320 \pm 0.028) - (0.125 \pm 0.013)i$	$0.328 - 0.129i$
$1/2+i$	$(0.297 \pm 0.030) - (0.160 \pm 0.019)i$	$0.300 - 0.163i$
$1/2+2i$	$(0.164 \pm 0.025) - (0.228 \pm 0.036)i$	$0.160 - 0.223i$
0	(0.467 ± 0.039)	0.478
$0+(1/4)i$	$(0.472 \pm 0.037) - (0.068 \pm 0.008)i$	$0.471 - 0.067i$
$0+(1/2)i$	$(0.449 \pm 0.035) - (0.129 \pm 0.016)i$	$0.451 - 0.132i$
$0+(3/4)i$	$(0.408 \pm 0.038) - (0.186 \pm 0.022)i$	$0.418 - 0.190i$
$0+i$	$(0.367 \pm 0.045) - (0.234 \pm 0.034)i$	$0.374 - 0.240i$
$0+2i$	$(0.242 \pm 0.032) - (0.407 \pm 0.071)i$	$0.150 - 0.308i$
$-1/2$	(0.627 ± 0.051)	0.645
$-1/2+(1/4)i$	$(0.638 \pm 0.054) - (0.101 \pm 0.014)i$	$0.635 - 0.101i$
$-1/2+(1/2)i$	$(0.620 \pm 0.047) - (0.197 \pm 0.028)i$	$0.605 - 0.198i$
$-1/2+(3/4)i$	$(0.588 \pm 0.057) - (0.307 \pm 0.044)i$	$0.554 - 0.288i$
$-1/2+i$	$(0.574 \pm 0.048) - (0.408 \pm 0.065)i$	$0.485 - 0.365i$
$-1/2+2i$	$(0.522 \pm 0.066) - (0.973 \pm 0.119)i$	$0.107 - 0.441i$

[a] Initial sample sizes for (15) are 64 paths and were cut down if $|x| > 10^6$. In this table $T = 100$, and statistical errors within the 64 paths showed $1/\sqrt{t}$ behavior.

degree of cancellation is required. The magnitude of the problem caused by such cancellations varies with the parameter σ which in turn has a strong influence on the distribution of β values in various solutions.

In the next section we illustrate the aproximate equality of (13) and

(15) (for a large finite time T) for the example of $A(x)=x^2$ by comparing the numerical integration[6] of (13) to the long-time average (15). The numerical solution of the stochastic differential equation (11) was computed by the method of Helfand.[7] We find agreement to a very satisfactory precision (see Table I).

2. NUMERICAL PROCEDURE AND RESULTS

We have diagonalized the eigenvalue equation $H\psi=\lambda\psi$ by computing the eigenvalues of the discretized problem

$$\sum_{j=0}^{N} H_{ij}a_j=\lambda a_i, \qquad 0\leqslant i\leqslant N \tag{24}$$

where the Rayleigh–Ritz expansion

$$\psi=\sum_{j=0}^{N} a_j\phi_j(x) \tag{25}$$

is in eigenvectors of the harmonic oscillator. The matrix elements

$$H_{ij}=\int dx\,\phi_i(x)H\,\phi_j(x)$$

were computed from the ladder operators

$$a=\frac{1}{\sqrt{2}}\left(x+\frac{\partial}{\partial x}\right), \qquad a^+=\frac{1}{\sqrt{2}}\left(x-\frac{\partial}{\partial x}\right)$$

We find that for the first few eigenvalues ($|\lambda|$ small), a few hundred terms in (25) are adequate provided $\operatorname{Re}\sigma>-1$. For $\operatorname{Re}\sigma\ll-1$, (25) becomes unreliable and N is prohibitively large.

In Fig. 1 we plot the modulus $|a_k|$ vs. k for the numerical solutions of the two lowest lying eigenstates when $\sigma=-\frac{1}{2}$ and $\sigma=-\frac{1}{2}+5i$. For these figures $N\leqslant 50$ is clearly sufficient.

A modified version of H. R. Swarz's algorithm BANDR[8] was used to reduce $[H_{ij}]$ to tridiagonal form. After reduction to tradiagonal form, a complex version of TQL1[9] yields the eigenvalues. It is known that complex versions of BANDR can be unstable for some problems.[10] We did careful comparisons of our results with those from the LR method[11] and are quite comfortable with the CBANDR procedure. The even and odd parts of matrix $[H_{ij}]$ each taken separately have bandwidth = 7; hence, an operation count proportional to $7N^2$ is clearly an advantage over LR with an operation count $O(N^3)$.

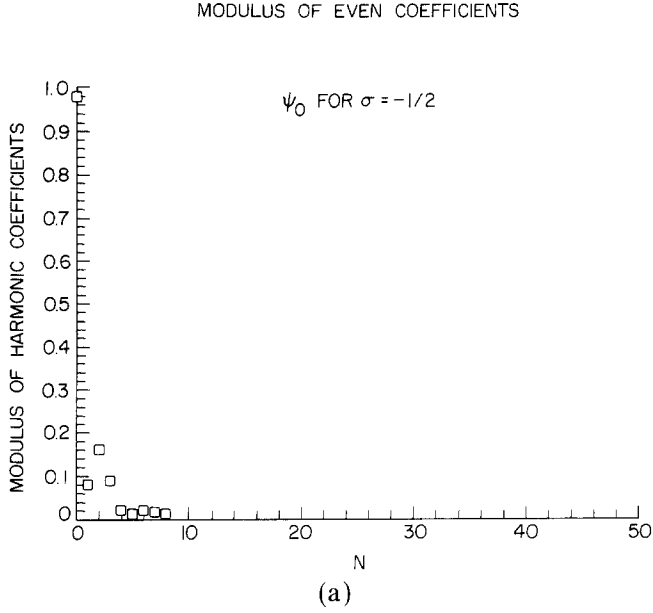

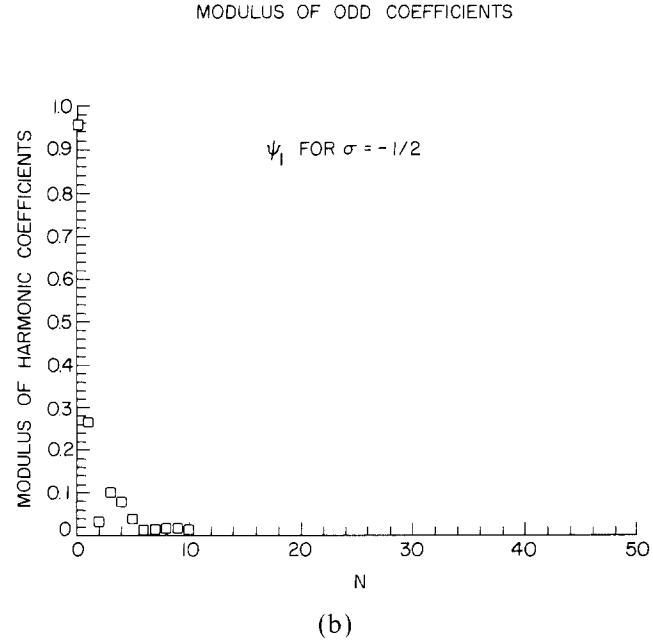

Fig. 1. Plots of modulus $|a_K|$ of harmonic oscillator coefficients in expansion (25), vs. k. Coefficients $|a_K| < 10^{-3}$ were ignored.

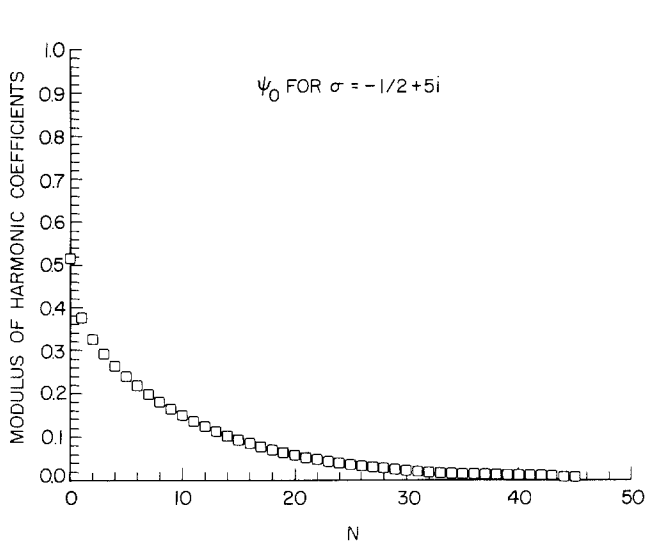

(c)

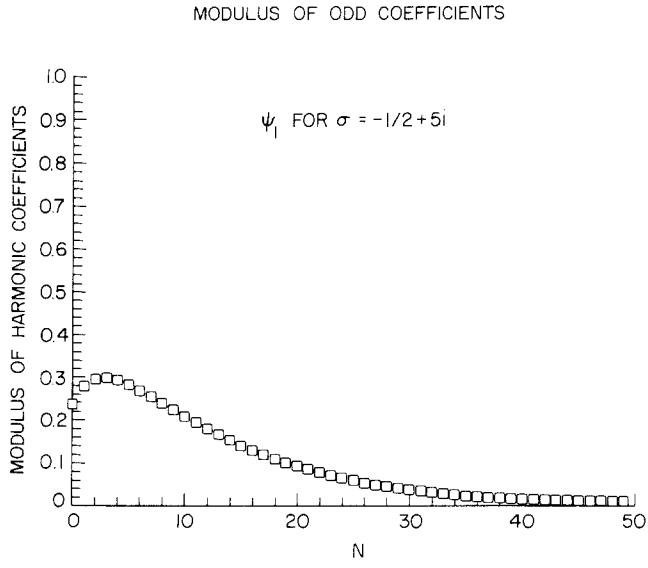

(d)

Fig. 1 (*continued*)

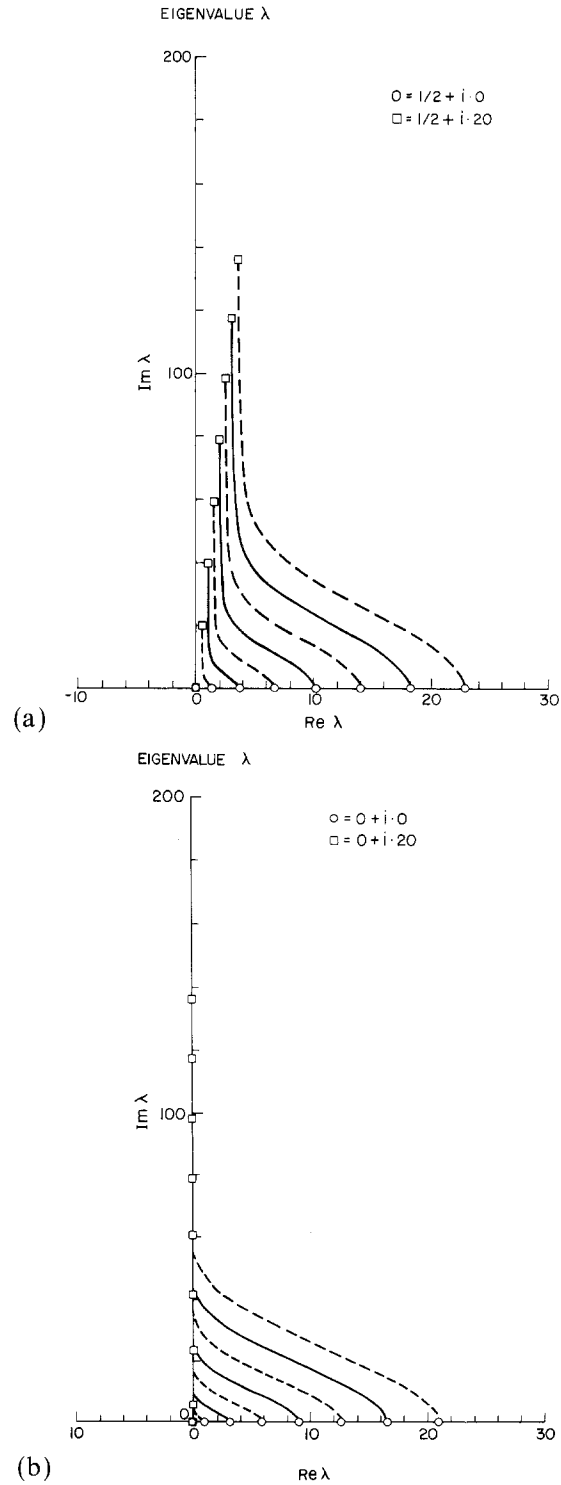

Fig. 2. Trajectories of the first eight eigenvalues of operator (23), for $0 \leqslant \operatorname{Im} \sigma \leqslant 20$. The even solutions are solid lines, odd solutions are dashed.

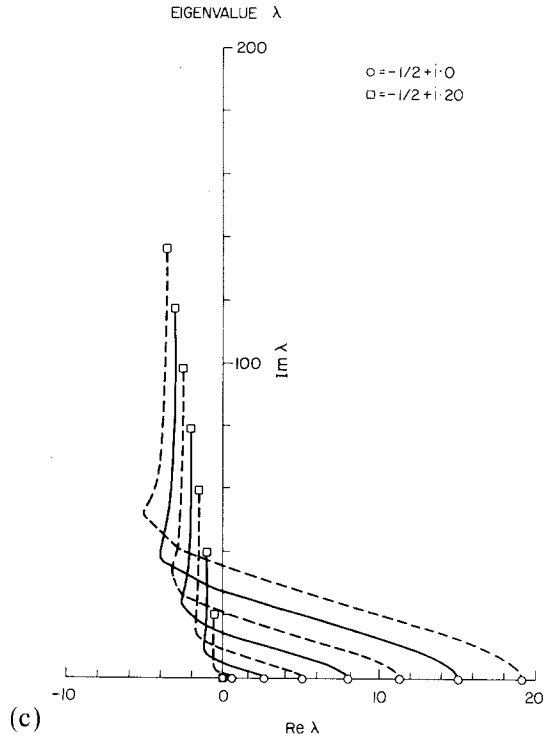

Fig. 2 (*continued*)

By scaling x in (23), $x \to \xi x$, the scaled eigenvalue equation

$$H_\xi \psi = \lambda_\xi \psi$$

can be made more stable than the original. Here $\lambda_\xi = \xi^2 \lambda$ and $H_\xi = \xi^2 H(\xi x)$. The choice $\xi^2 = 1/|\sigma|$ seemed best.

The trajectories of the first eigenvalues of (24) for $0 \leqslant \operatorname{Im} \sigma \leqslant 20$ are shown in Figs. 2. Note that for large $\operatorname{Im} \sigma$ that the successive eigenvalues fall on a straight line. In the following section we show that this "complex frequency" harmonic oscillator result is not surprising.

The coefficients a_j were computed by finding the null vector of $[H_{ij}] - \lambda$. For this computation the condition number estimator CGBCO from Linpack[22] was used. We found condition numbers greater than 10^{14}.

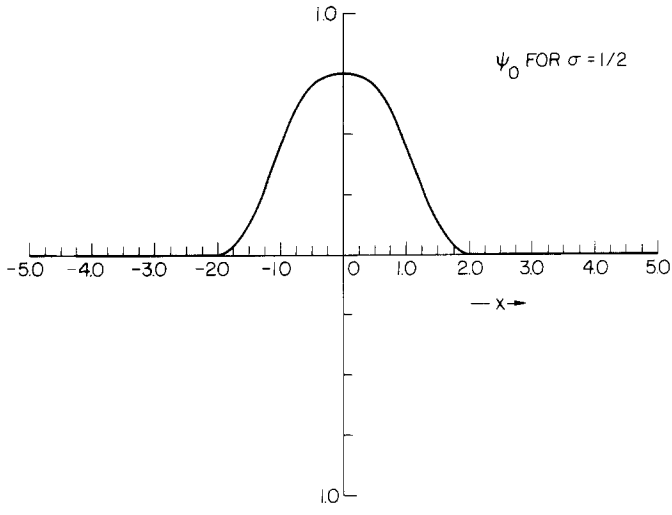

(a)

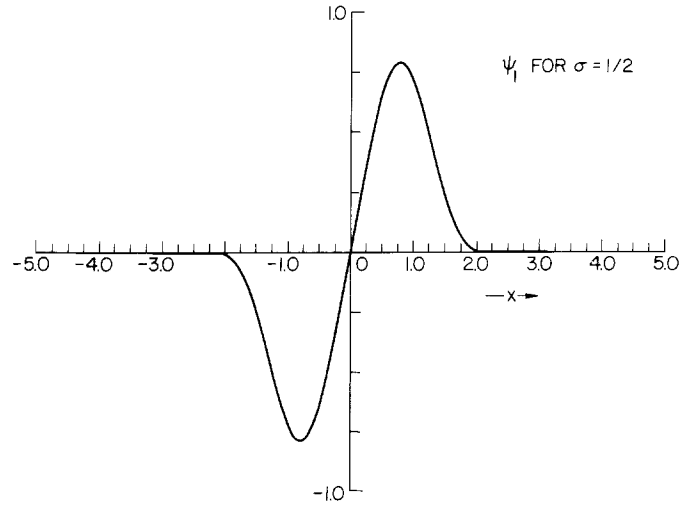

(b)

Fig. 3. Plots of the first two eigenfunctions of operator (23) in x space when Re $\sigma = \frac{1}{2}, 0, -\frac{1}{2}$. The real parts are plotted as solid lines, imaginary parts as dashed lines. The phase convention is described in the text of Section 2.

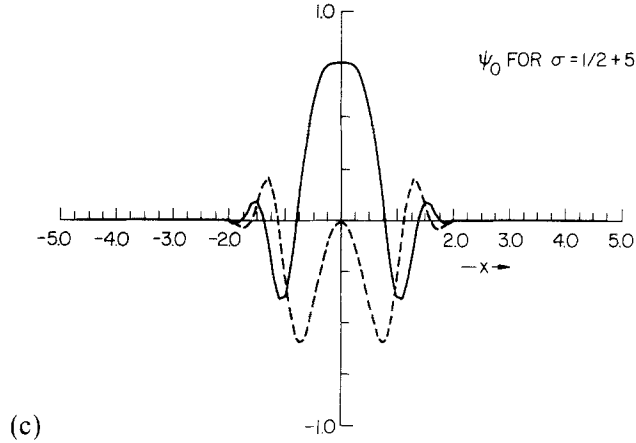

(c)

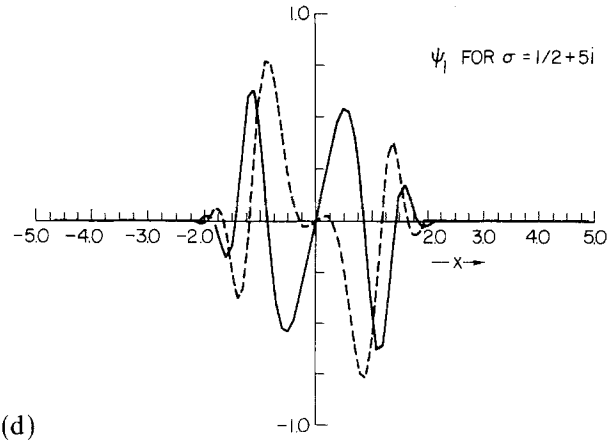

(d)

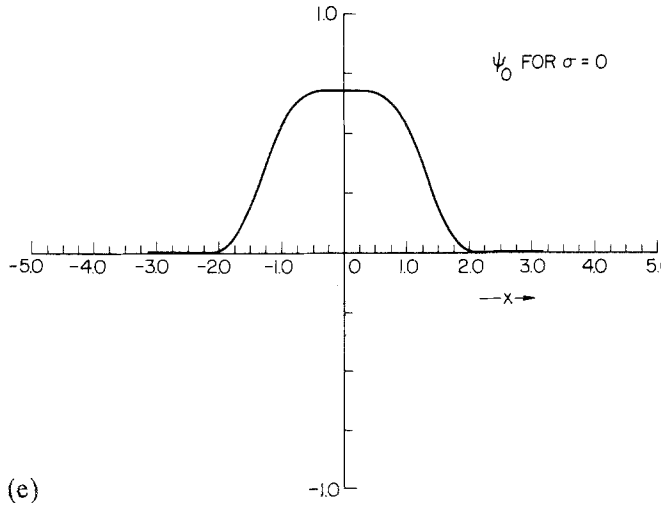

(e)

Fig. 3 (*continued*)

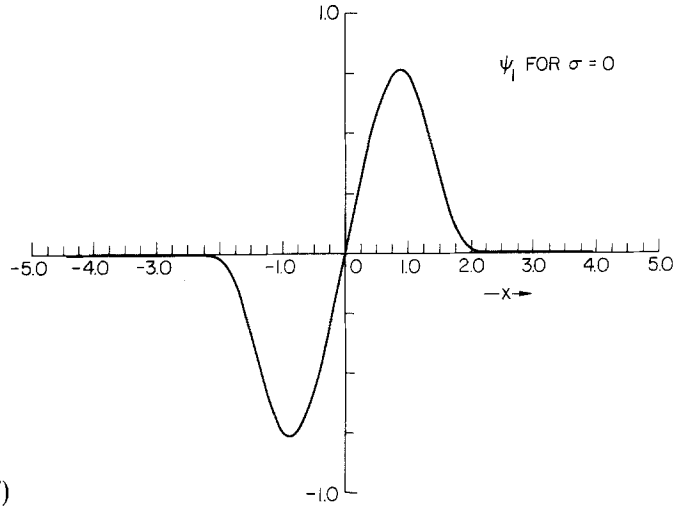

(f)

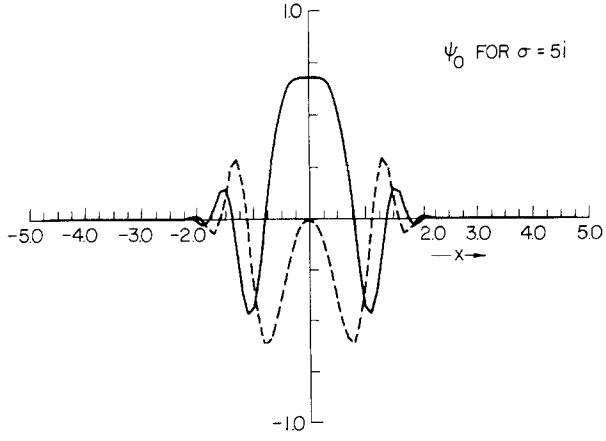

(g)

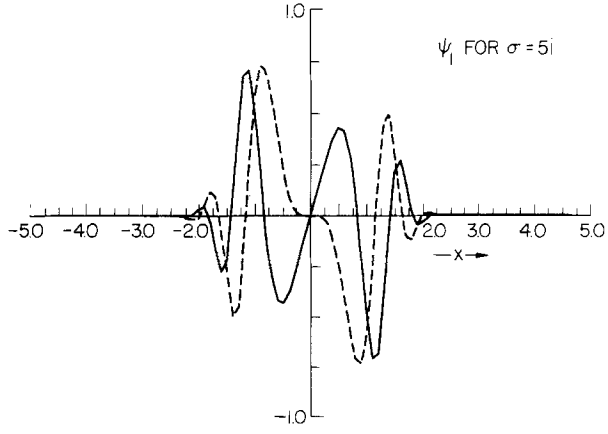

(h)

Fig. 3 (*continued*)

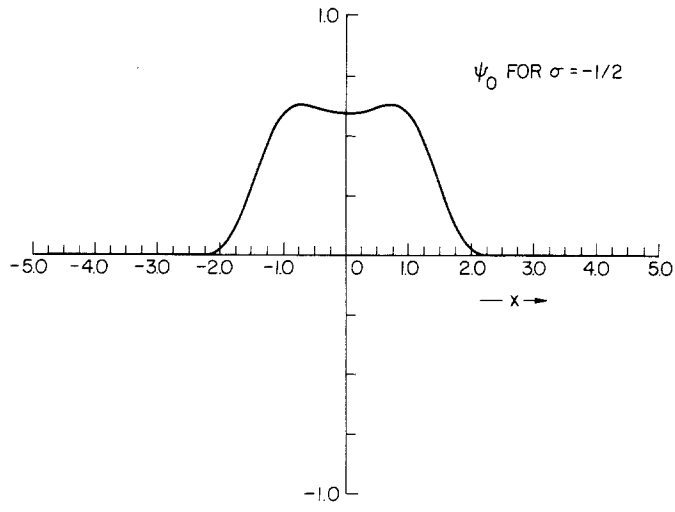

(i)

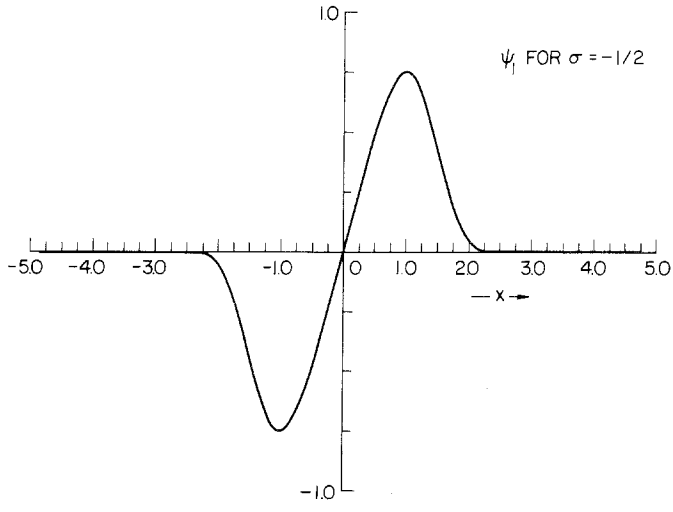

(j)

Fig. 3 (*continued*)

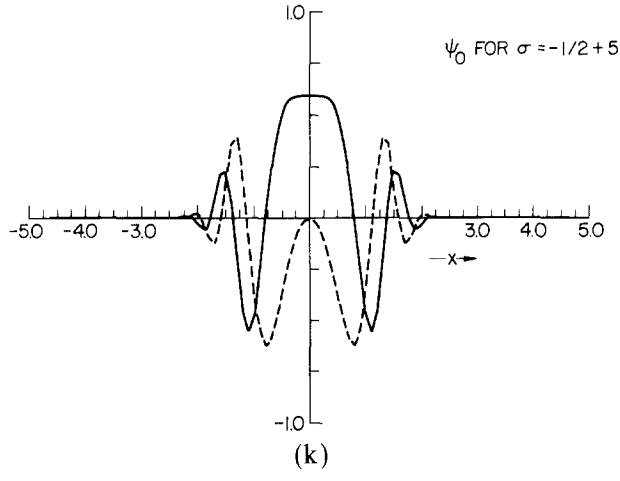

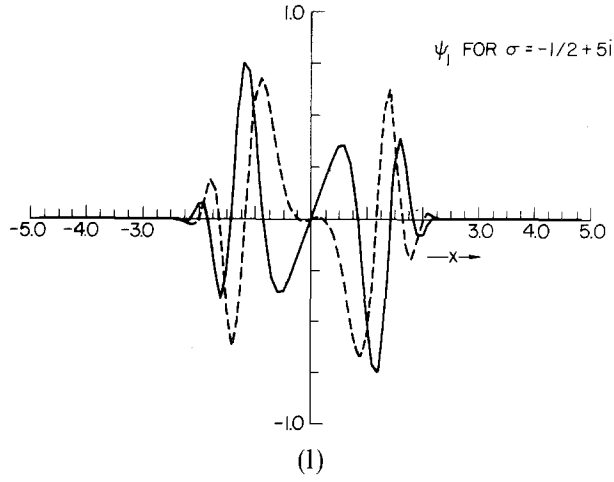

Fig. 3 (*continued*)

Furthermore, the eigenvalues from TQL1 were compared with inner products

$$\sum_{i,j} a_i^* H_{ij} a_j \Big/ \sum_i a_i^* a_i$$

and gave excellent agreement.

In Figs. 3 we illustrate the wave functions for the first two eigenvalues. Comparing 3^a, 3^e, and 3^i, note the bifurcation in the ground state at the

critical point $\operatorname{Re}\sigma = 0$.[13] The phase of these wave functions were chosen such that $\operatorname{Im}\psi_0(x=0)=0$. Namely, a phase α was chosen such that

$$\operatorname{Im}(e^{i\alpha}\psi_0(x=0))=0$$

and every other ψ_λ was multiplied by this same phase factor $e^{i\alpha}$. The real parts of ψ are shown in solid lines, the imaginary parts are dashed.

2.1. Large-σ Results

In Fig. 2 we have shown numerical evidence for $\operatorname{Re}\sigma \geqslant 0$ that $\operatorname{Re}\lambda \geqslant 0$. Apparently for large $|\sigma|$ the spectrum is given by the "complex frequency" harmonic oscillator result $\lambda = n\sigma$. Equation (23) takes the form of a complex frequency harmonic oscillator when $|\sigma|$ is large. If $\operatorname{Re}\sigma \leqslant 0$, however, the solutions are not obviously square integrable. Our example is

$$H\psi = -\frac{1}{2}\left(\frac{\partial}{\partial x} - g\right)\left(\frac{\partial}{\partial x} + g\right)\psi = \lambda\psi \tag{26}$$

where $g = (1/2)(\partial S/\partial x) = \sigma x + x^3$. The ground state ψ_0 satisfies $(\partial_x + g)\psi_0 = 0$ and is

$$\psi_0(x) = \exp\left(\frac{-\sigma x^2}{2} - \frac{x^4}{4}\right)$$

Now, for large x, (26) is approximately

$$\frac{1}{2}\left(-\frac{\partial^2}{\partial x^2} + x^6\right)\psi \cong 0$$

Asymptotically $|\psi| \sim \exp(-x^4/4)$. We are therefore tempted to write all solutions of (26) as

$$\psi(x) = \phi(x)\,\psi_0(x)$$

with the requirement that ϕ be regular. The eigenvalue problem for ϕ is

$$-\frac{1}{2}\frac{\partial^2\phi}{\partial x^2} + (\sigma x + x^3)\frac{\partial\phi}{\partial x} = \lambda\phi \tag{27}$$

For large $|\sigma|$, noting from Figs. 2 that $\lambda(\sigma)$ is growing, (27) becomes

$$\sigma x\frac{\partial\phi}{\partial x} = \lambda\phi$$

Table II. The Ratio $|\int e^{-s}\,dx|/\int |e^{-s}|\,dx$ Illustrating Cancellation in the Complex Measures

Contributions from complex measures	
σ	$\dfrac{\lvert\int_{-\infty}^{\infty} e^{-S(x)}\,dx\rvert}{\int_{-\infty}^{\infty} \lvert e^{-S(x)}\rvert\,dx}$
2	1.0
$2+i$	0.970
$2+2i$	0.892
$2+3i$	0.803
$2+4i$	0.723
1	1.0
$1+i$	0.942
$1+2i$	0.813
$1+3i$	0.690
$1+4i$	0.600
0	1.0
$0+i$	0.880
$0+2i$	0.657
$0+3i$	0.503
$0+4i$	0.423
$-1/2$	1.0
$-1/2+i$	0.824
$-1/2+2i$	0.531
$-1/2+3i$	0.379
$-1/2+4i$	0.318

having solution $\phi \propto x^{\lambda/\sigma}$. For ϕ to be regular along the negative x axis requires $\lambda = n\sigma$, n a positive integer.

2.2. Stochastic Estimate of $\bar{A}$

In Table I we tabulate the evaluation of (13) and (15) for a finite T for the special case of $A = x^2$. The stochastic data were obtained for $T = 10^2$ and by averaging the results over as many as 64 different sample paths. Any path that diverged was thereafter dropped from the sample. For $\mathrm{Re}\,\sigma \geqslant \frac{1}{2}$ no more than one path diverged, for $\mathrm{Re}\,\sigma = 0$ as many as half the paths diverged, and for $\mathrm{Re}\,\sigma = -\frac{1}{2}$ only a few paths survived.

From our numerical results about the spectrum of (8), we expect that for $\mathrm{Re}\,\sigma > 0$ the results of (13) and (15) for a large finite T should be approximately equal. Indeed, they seem to be so. Errors in the

stochastically determined results fell as $T^{-1/2}$ and showed a remarkable independence of sample size. Additional accuracy may be attained for $\operatorname{Re}\sigma \geqslant \frac{1}{2}$ simply by increasing T which is easily done since almost no path diverges in that case; in some examples we have used $T = 10^3$ or even 10^4 with correspondingly improved accuracy and with almost no path divergences. These data are not quoted for lack of an across-the-board comparison.

As one measure of the cancellation occurring in the complex integrands we list in Table II the ratio of complex measures given by

$$\frac{|\int dx\, e^{-S(x)}|}{\int dx\, |e^{-S(x)}|}$$

3. CONCLUSIONS

In summary, we have demonstrated that reasonably accurate numerical estimates of averages such as (13) may be computed by long-time averages involving solutions of an associated Langevin equation (11) even when the distribution (e^{-S}) is complex, provided the convergence criterion (2) is satisfied. The accuracy that may be attained with this method increases the more rapidly the convergence criterion (2) is obeyed. Although the example we have considered here is only one-dimensional ($x \in \mathbb{R}$) the method is applicable to N-dimensional examples ($x \in \mathbb{R}^N$); for example, the model treated in Ref. 3 took N as great as 2048. Our purpose in this paper has been to give a more in-depth study of the principles of the complex Langevin method rather than deal with a complicated many-dimensional model. Finally, we observe that the property $\operatorname{Re}\lambda_n > 0$, $n \geqslant 1$ for $\operatorname{Re}\sigma > 0$—as is strongly evident from the numerical studies for the example of this paper—appears sufficiently simple in character to admit an analytic proof. Unfortunately we have been unsuccessful in that quest.

ACKNOWLEDGMENTS

The authors would like to thank L. C. Kaufman for the use of CBANDR and for discussions about using the condition number estimates for computing selected eigenvectors. We would also like to thank E. Balslev, A. Devinatz, A. Friedman, J. Jerome, L. Shepp, and L. E. Thomas for their interest in this problem.

REFERENCES

1. N. G. Van Kampen, *Stochastic Processes in Physics and Chemistry* (North-Holland, Amsterdam, 1981); P. T. Soong, *Random Differential Equations in Science and Engineering* (Academic Press, New York, 1973).
2. J. R. Klauder, in *Recent Developments in High-Energy Physics*, H. Mitter and C. B. Lang, eds. (Springer-Verlag, Vienna, 1983), p. 251.
3. J. R. Klauder, *Phys. Rev. A* **29**:2036 (1984).
4. T. Kato, *Perturbation Theory for Linear Operators* (Springer, New York, 1966).
5. B. Simon, *Functional Integrals and Quantum Physics* (Academic, New York, 1979).
6. R. Piessens, E. De Doncker-Kapenga, C. W. Uberhuber, and D. K. Kahaner, *QUADPACK—A Subroutine Package for Automatic Integration* (Springer-Verlag, Berlin, 1983), routines QAWF and QAGI.
7. E. Helfand, *Bell Syst. Tech. J.* **58**(10):2289 (1979); see also H. S. Greenside and E. Helfand, *Bell. Syst. Tech. J.* **60**(8):1927 (1981).
8. H. R. Schwarz, *Numer. Math.* **12**:231–241 (1968); J. H. Wilkinson and C. Reinsch, *Handbook for Automatic Computation, Vol. II, Linear Algebra* (Springer, New York, 1971), p. 273.
9. H. Bowdler, R. S. Martin, C. Reinsch, and J. H. Wilkinson, *Numer. Math.* **11**:293–306 (1968); J. H. Wilkinson and C. Reinsch, *Numer. Math.* **11**:227 (1968).
10. J. Cullem and R. Willoughby, *J. Comput. Phys.* **44**(2):329–358 (December 1981).
11. R. S. Martin and J. H. Wilkinson, *Numer. Math.* **12**:349–368 (1968); J. H. Wilkinson and C. Reinsch, *Numer. Math.* **12**:339 (1968); Numerical Algorithms Group (NAG version 9) library routines FO1AMF and FO2ANF.
12. J. J. Dongarra, C. B. Moler, J. R. Bunch, and G. W. Stewart, *LINPACK Users Guide* (SIAM Publication, Philadelphia, 1979).
13. E. Knobloch and K. A. Wiesenfeld, *J. Stat. Phys.* **33**(3):611 (1983).